LWT - Food Science and Technology 111 (2019) 520–526

Contents lists available at ScienceDirect

LWT - Food Science and Technology

journal homepage: www.elsevier.com/locate/lwt

Functional and structural effects of hydrocolloids on Ca(II)-alginate beads containing bioactive compounds extracted from beetroot

Tatiana Rocio Aguirre Calvo[a,b], Patricio R. Santagapita[a,b,*], Mercedes Perullini[c,d,**]

[a] Universidad de Buenos Aires, Facultad de Ciencias Exactas y Naturales, Departamentos de Industrias y Química Orgánica, Buenos Aires, Argentina
[b] CONICET-Universidad de Buenos Aires, Instituto de Tecnología de Alimentos y Procesos Químicos (ITAPROQ), Buenos Aires, Argentina
[c] Universidad de Buenos Aires, Facultad de Ciencias Exactas y Naturales, Departamento de Química Inorgánica, Analítica y Química Física, Buenos Aires, Argentina
[d] CONICET-Universidad de Buenos Aires. Instituto de Química Física de los Materiales, Medio Ambiente y Energía (INQUIMAE), Buenos Aires, Argentina

ARTICLE INFO

Keywords:
Antioxidants
Betalains
Hydrogels
Biopolymers
Microstructure
SAXS

ABSTRACT

In the present research, valuable bioactives such as betacyanin and polyphenols of beetroot leaf and stem (a food waste) were extracted and encapsulated in Ca(II)-alginate beads, using sucrose, arabic and guar gums, and low and high methoxyl pectins as excipients. A complete SAXS evaluation from the molecular to the supramolecular changes (1–100 nm) produced by excipients and extracts on the microstructure of the hydrogel network was performed. Thus, combining structural-functional information allows for the design of Ca(II)-alginate systems based not only on functional aspects. Here we demonstrate that the presence of hydrocolloids affected the alginate dimers size and density, the rods size and compactness as well as their interconnectivity. Nevertheless, these modifications can be overlied by the presence of an extract, which leads to alginate coordination prior to gelation, strongly affecting the resulting microstructure. Among the used hydrocolloids, only guar gum achieves the two proposed criteria: increasing functional properties and generating stable microstructural modulations.

1. Introduction

The encapsulation process consists of the incorporation of food ingredients, enzymes, cells or other biocompounds in a matrix to preserve their stability and protect them against environmental stresses over extended periods (Galanakis, 2012; Quintanilla-Carvajal et al., 2010). The encapsulation must be designed to form a barrier between the internal phase and its surroundings by using a protective wall or matrix agents (Wandrey, Bartkowiak, & Harding, 2010). The rapid and consolidated formation of an alginate gel in the presence of calcium ions and the relative gentle gelation process as well as the elucidation of structure-function relationships of this versatile material explains its increasing use for the immobilization of biological compounds (Aguirre Calvo, Busch, & Santagapita, 2017 and, 2018; Thu et al., 2000; Ćujić et al., 2016; Deladino, Navarro, & Martino, 2013; Traffano-Schiffo, Castro-Giraldez, Fito, Perullini, & Santagapita, 2018, 2017; Vicini, Castellano, Mauri, & Marsano, 2015).

Co-materials such as sugars and hydrocolloids provide additional advantages in Ca(II)-alginate systems. It has been demonstrated that the addition of guar gum increases the entrapment efficiency of alginate–guar gum hydrogels used in drug delivery as matrix forming material (George & Abraham, 2007; Krishnaiah, Karthikeyan, & Satyanarayana, 2002) and improves the activity of an entrapped enzyme in operational conditions (Traffano-Schiffo et al., 2018). The combination of alginate-arabic gum has been used for the protection of probiotic bacteria, vegetable extract and drugs during drying, storage, and in the gastric tract (Nami, Haghshenas, & Yari Khosroushahi, 2016; Nayak, Das, & Maji, 2012; Tsai, Kitamura, & Kokawa, 2017). Encapsulation in alginate-high methoxyl pectin hydrogel significantly reduced the photodegradation rate of bioactive compounds (Guo, Giusti, & Kaletunç, 2018). Moreover, the combined use of alginate with low methoxyl pectin improves microbeads mechanical properties (Bekhit et al., 2018). Therefore, new formulations incorporating guar gum, arabic gum, low methoxyl and high methoxyl pectin have been studied, in order to improve the loading efficiency and protect bioactive compounds.

Bioactives from food waste can be extracted and used for the development of nutraceuticals and functional food additives (Kumar, Yadav, Kumar, Vyas, & Dhaliwal, 2017; Silveira, Daroit, & Brandelli, 2008; Wilkins, Widmer, Grohmann, & Cameron, 2007). It was reported

* Corresponding author. CONICET-Universidad de Buenos Aires, Instituto de Tecnología de Alimentos y Procesos Químicos (ITAPROQ), Buenos Aires, Argentina.
** Corresponding author. Universidad de Buenos Aires, Facultad de Ciencias Exactas y Naturales, Departamento de Química Inorgánica, Analítica y Química Física, Buenos Aires, Argentina.
E-mail addresses: prs@di.fcen.uba.ar (P.R. Santagapita), mercedesp@qi.fcen.uba.ar (M. Perullini).

https://doi.org/10.1016/j.lwt.2019.05.047
Received 7 January 2019; Received in revised form 29 April 2019; Accepted 9 May 2019
Available online 11 May 2019

that food waste can contain high values of polyphenols concentration which have antioxidant activity and diminish the risk of developing certain types of cancer (Baiano, 2014; Day, Seymour, Pitts, Konczak, & Lundin, 2009). The growing demand for daily intake of fruits and vegetables has generated a greater global consumption guiding to a healthy diet. Beetroot (*Beta vulgaris*) is considered a source of vitamins, minerals and biocompounds such as polyphenols and betalains (Baiao et al., 2017; Jackman & Smith, 1996; Sawicki & Wiczkowski, 2018). Despite being a vegetable of mass consumption around the world it is usually commercialized without stems or leaves, in most cases being discarded or used as organic fertilizers and animal feed (Amaral, Anghinoni, & Deschamps, 2004; Mello, Franzolini, Fernandes, Franco, & Alves, 2008). Stems and leaves become a sub-product of high nutritional and chemical value being wasted.

Approaches have been pursued to analyze the structure and morphology of the associations of alginate chains to reveal structure-function relationships. Small-angle X-ray scattering (SAXS) is a non-invasive technique that has proven to be an accurate and powerful tool for exploring the nanoscale morphology of hydrogels. It reveals subtle differences in electron density within the reticulated networks of hydrogels in the range of 1–100 nm, providing information on the supramolecular structure formed by biopolymers (Traffano-Schiffo et al., 2018; Wu et al., 2018). Ca(II)-alginate structure can be modulated with the addition of different encapsulating agents, in order to tune properties such as mechanical strength or leakage of entrapped biomolecules (Aguirre Calvo et al., 2017; Chawda, Shi, Xue, & Young Quek, 2017; Santagapita, Mazzobre, & Buera, 2011). Moreover, the possible structural changes are driven not only by the presence of excipients adhered to the Ca(II)-alginate structure but also by the presence of extracts. Changes in certain microstructural parameters go from the molecular (arrange of alginate polymer dimers) to the supramolecular (interconnection of the rods composing the microstructure of the hydrogel) structure of Ca(II)-alginate beads (Aguirre-Calvo, Perullini, & Santagapita, 2018; Traffano-Schiffo, Aguirre Calvo, Castro-Giraldez, Fito, & Santagapita, 2017).

In the present research, efforts are gathered to recover valuable bioactives from food waste and encapsulate them in Ca(II)-alginate beads, using sucrose, arabic and guar gums, and low and high methoxyl pectins as excipients. The subsequent evaluation performed by SAXS analysis shed light on changes produced by excipients and extracts from the molecular to the supramolecular microstructure of the hydrogel network. At the same time, it provides a valuable solution to the preparation of nutraceuticals not only considering functional aspects as loading efficiency and remaining antioxidant activity, but also combining structural-functional information leading to the development of improved Ca(II)-alginate beads.

2. Materials and methods

Materials employed are listed below: sodium alginate (Algogel 5540) from Cargill S.A. (San Isidro, Buenos Aires, Argentina), molecular weight of 1.97 (± 0.06)·10^5 g/mol and mannuronate/guluronate ratio of 0.6; D(+) Sucrose p.a. (A.C.S) (Biopack, Zárate, Buenos Aires, Argentina) molecular weight of 342.30 g/mol; guar gum (Cordis S.A., Villa Luzuriaga, Buenos Aires, Argentina), molecular weight of 2.2 (± 0.1)·10^5 g/mol and a mannose/galactose ratio of 1.8; arabic gum (Biopack, Zárate, Buenos Aires, Argentina), molecular weight of 2.5 (± 0.1)·10^5 g/mol and a purity of 99%; low methoxyl pectin (Degusta Meath & Nutrition Argentina S.A. Bs. As. Argentina) esterification degree between 26 and 31%; and high methoxyl pectin (Cargill Inc., Mineapolis, Minnesota, USA). Table 1 summarizes relevant physicochemical properties of each biopolymer. Leaf and stem extract from beetroot were prepared according to Aguirre-Calvo et al., 2018. Briefly, leaves and stems were scalded, mixed in a blender with water (1:2) for 5 min at 20 °C and then centrifuged at 10,000 rpm for 30 min at 5 ± 1 °C. Samples were kept in the dark at 4 ± 1 °C until used.

Table 1
Physicochemical properties of hydrocolloids used as excipients in Ca(II)-alginate beads.

Hydrocolloids	Mv	Molecular structure	Zeta-Potential (mV)	Principal Properties	Intrisic viscosity
Guar gum	1935 kDa (Cheng, Brown, & Prud'homme, 2002)	Galactomannan (1–4)-linked β-D-mannopyranose backbone with branch points from their 6-positions linked to α-D-galactose (that is, 1- > 6-linked-α-D-galactopyranose).	−6.3 (Pal el al., 2016)	Thickener Non-gelling agent Stabilizer, water retention	16.39 dl/g (Cheng et al., 2002)
Arabic gum	845 kDa (Gómez-Díaz, Navaza, & Quintáns-Riveiro, 2008)	Mixture of arabinogalactan oligosaccharides, polysaccharides, and glycoproteins.	−9.4 (Campelo et al., 2017	High Emulsification properties, Thickener	0.18 ± 0.01 dl/g (Gómez-Díaz et al., 2008)
Low methoxyl pectin (LMP)	76 ± 4 kDa (28% methoxylated) (Yapo & Koffi, 2013)	α-(1–4)-linked D-galacturonic acid polysaccharide backbone. HMP (> 50% esterified) LMP (< 50% esterified)	−4.0 (Opanasopit, Apirakaramwong, Ngawhirunpat, Rojanarata, & Ruktanonchai, 2008)	Gelation, thickener, Thermoirreversible gels in the presence of calcium ions.	2.87 ± 0.04 dl/g (Yapo & Koffi, 2013)
High methoxyl pectin (HMP)	80 ± 3 kDa (70% methoxylated) (Sayah et al., 2016)		−7.6 (Zhao et al 2013)	Thickener, stabilizer Thermally irreversible gels in presence of a minimum amount of soluble solids (> 55%) and acid pH (~ 3-3.5).	2.5 ± 0.1 dl/g (Sayah et al., 2016)

2.1. Bioactive extract encapsulation: Ca(II)-alginate bead generation

Aqueous extract of leaf or stem were mixed with 10 g kg^{-1} of sodium alginate and 200 g kg^{-1} of sucrose (AS) and then stirred until complete dissolution. Formulations were prepared by adding the alginate-sucrose solution with 2.5 g kg^{-1} of four different hydrocolloids, generating the following systems: alginate-sucrose-guar gum (ASGG); alginate-sucrose-arabic gum (ASAG); alginate-sucrose-LM pectin (ASL); alginate-sucrose-HM pectin (ASH). Each formulation is then dropped with a needle (Novofine 31G, 0.25 mm diameter) with a peristaltic pump at 9.0 ± 0.1 rpm (model BT50-1J-JY10, Boading Longer Precision Pump Co, Ltd, China), on 25 g kg^{-1} $CaCl_2$ solution with 200 g kg^{-1} of sucrose (Cicarelli S.A., Argentina) in 0.1 M acetate buffer pH 5.5. The distance between the needle and the $CaCl_2$ solution was 6.0 ± 0.1 cm. After beads generation, they were maintained for 5 min in $CaCl_2$ solution and then washed 2 times (for 5 s each wash) with bidistilled cold water, obtaining beads of Feret's diameter = 1.6 ± 0.1 mm. Beads were kept at 5 ± 1 °C until its use. Control beads without extracts were also produced following the same conditions for comparative purposes.

2.1.1. Loading efficiency of betacyanins

Loading efficiency of betacyanins was calculated based on the spectrophotometrically quantification by Aguirre-Calvo et al. (2018). Briefly, concentrations obtained from absorbance readings of 30 beads mixed previously with 0.175 mL of 100 g kg^{-1} sodium citrate by means of a spectrophotometer (JASCO Inc., Maryland, USA), $[BC]_{beads}$, were related to the concentration of main extract, $[BC]_{extract}$, as described in equation (1) (eq (1)).

$$L.E(bc) = \left(\frac{[BC]_{beads}}{[BC]_{extract}}\right) * 100 \quad (1)$$

As described in Aguirre-Calvo et al., 2018, the concentration of betacyanins in the beads, $[BC]_{beads}$, was calculated taking into account the size and number of beads used in the determination, considering the volume $Vol_{bead} = \frac{3}{4}\pi r^3$ for each of the systems, where [r] is the half of the Feret's diameter, and the dilution factor in the sodium citrate solution used for liquefaction. Thus, the $[BC]_{beads}$ values are expressed as mg_{BC}/mL of liquefied beads and can be compared to the concentration of BC in the extract, $[BC]_{extract}$.

2.1.2. Loading efficiency of polyphenols

The loading efficiency of polyphenols was calculated following Aguirre-Calvo et al. (2018) based on total polyphenols content of the beads ($[TP]_{beads}$) related to the concentration of main extract ($[TP]_{extract}$), following equation (2) (eq (2)). Concentration was calculated with the technique of Singleton et al. (1999) using Folin Ciocalteau reagent (Biopack®, Zárate, Buenos Aires, Argentina). Briefly, 30 beads were mixed previously with 0.175 mL of 100 g kg^{-1} sodium citrate. Then, 125 μL of a solution of Na_2CO_3 (200 g kg^{-1}), 800 μL of distilled water and 50 μL of sample (disintegrated beads or extracts) were added to 125 μL of the Folin Ciocalteau reagent. The absorbance at 765 nm was measured after 30 min of reaction at 40 °C in the dark. Results were expressed as mg $_{GAE}$/mL through a calibration curve, being GAE: gallic acid equivalents.

$$L.E(polyphenols) = \left(\frac{[TP]_{beads}}{[TP]_{extract}}\right) * 100 \quad (2)$$

As described in Aguirre-Calvo et al., 2018, the total polyphenol content of the beads, $[TP]_{beads}$, was calculated taking into account the size and number of beads used in the determination, considering the volume $Vol_{bead} = \frac{3}{4}\pi r^3$ for each of the systems, where [r] is the half of the Feret's diameter and the dilution factor in the sodium citrate solution used for liquefaction. Thus, the $[TP]_{beads}$ values are expressed as mg_{GAE}/mL of liquefied beads and can be compared to the concentration of TP in the extract, $[TP]_{extract}$.

2.1.3. Remaining antioxidant activity by $ABTS^{\bullet+}$ radical

Remaining antioxidant activity was calculated by detecting the ability of the beads ($[AnA]_{beads}$) to scavenge the $ABTS^{\bullet+}$ free radical related to the extract ($[AnA]_{extract}$), as reported in equation (3) (eq (3)). Antioxidant activities of the samples were analyzed by ability to scavenge the $ABTS^{\bullet+}$ free radical using a modified methodology previously reported by Re, Pellegrini, Proteggente, Pannala, & Yang, 1999 and Aguirre-Calvo et al., 2018. Thirty beads were mixed with 0.175 mL of 100 g kg^{-1} sodium citrate; then 100 μL of the sample (liquefied beads or extracts) were mixed with 1.9 mL of activated $ABTS^{\bullet+}$ (7.0 mM ABTS previously mixed with 2.45 mM potassium persulfate and left for 16 h in the dark). Samples were measured at 734 nm after incubation at 30 °C for 30 min in a water bath. The percentage of inhibition was calculated against a control sample (without extracts) and compared to a gallic acid standard curve and expressed as mg_{GAE}/mL (Wootton-Beard, Moran, & Ryan, 2011). The $ABTS^{\bullet+}$ remaining antioxidant activity was calculated:

$$R.A.A.(ABTS^{\bullet+}) = \left(\frac{[AnA]_{beads}}{[AnA]_{extract}}\right) * 100 \quad (3)$$

As described in Aguirre-Calvo et al., 2018, the antioxidant activity of the beads, $[AnA]_{beads}$, was calculated taking into account the size and number of beads used in the determination, considering the volume $Vol_{bead} = \frac{3}{4}\pi r^3$ for each of the systems, where [r] is the half of the Feret's diameter, and the dilution factor in the sodium citrate solution used for liquefaction. Thus, the $[AnA]_{beads}$ values are expressed as mg_{GAE}/mL of liquefied beads and can be compared to the antioxidant activity of the extract, $[AnA]_{extract}$.

2.2. Fe^{3+} determination

Extract samples (10.00 mL) were brought to ashes and diluted with 10 mL of 1M HCl, then filtered. The supernatant was mixed (1:1) with 1M of ammonium thiocyanate for 15 min to generate the iron(III) complex. An external calibration curve was prepared by taking known amounts of standard Fe(III) solution (ferric ammonium sulfate). Absorbance was monitored at 490 nm. Results are expressed as mg of Fe^{3+} per kg of fresh sample (Chemteach, 2019).

2.3. Beads characterization

2.3.1. Macrostructural characterization

Area, perimeter, circularity and Feret's diameter described the macrostructural characterization of the beads. As described by Aguirre Calvo and Santagapita (2016), thirty beads were analyzed through digital analysis of images captured with a digital camera coupled to a binocular microscope and analyzed by the free license software ImageJ (http://rsbweb.nih.gov/ij/) by applying the “analyze particle” command of the software.

2.3.2. Microstructure characterization

The microstructure characterization was performed at the LNLS SAXS2 beamline in Campinas, Brazil, working at λ = 0.1488 nm with a vector (q) range of $0.096\,nm^{-1} < q < 2.856\,nm^{-1}$. All the parameters were analyzed as described in Traffano-Schiffo et al., 2018 and Aguirre-Calvo et al., 2018.

2.4. Statistical analyses

The statistical analyses were performed by one-way ANOVA with Tukey's post-test by using Prism 6.01 (GraphPad Software Inc., San Diego, CA, USA) in order to determine significant differences between the mean values of beads of different compositions on the measured

Table 2
Loading efficiencies of betacyanin ($L.E._{BC}$) and polyphenols ($L.E._{TP}$) and remaining antioxidant activity (RAA) of different formulations of Ca(II)-alginate-sucrose beads containing leave or stem extracts.

		$L.E_{BC}$ (%)	$L.E_{TP}$ (%)	$RAA_{(ABTS)}$ (%)
Leaf extract	AS	26.6 ± 0.2 ^{c,A}	38 ± 4 ^{b,B}	22 ± 4 ^{a,B}
	ASGG	35.1 ± 0.3 ^{a,A}	47 ± 1 ^{a,B}	26 ± 4 ^{a,B}
	ASAG	15.46 ± 0.01 ^{e,A}	28 ± 2 ^{c,B}	20 ± 2 ^{a,B}
	ASL	21.6 ± 0.4 ^{d,A}	37 ± 2 ^{b,B}	10 ± 2 ^{b,B}
	ASH	28.7 ± 0.2 ^{b,A}	38 ± 2 ^{b,B}	7 ± 2 ^{b,B}
Stem extract	AS	10.6 ± 0.4 ^{c,B}	58.2 ± 0.3 ^{ab,A}	48 ± 9 ^{b,A}
	ASGG	25.7 ± 0.4 ^{a,B}	60 ± 1 ^{a,A}	66 ± 3 ^{a,A}
	ASAG	20 ± 3 ^{b,A}	43.3 ± 0.9 ^{c,A}	38 ± 2 ^{b,A}
	ASL	21 ± 2 ^{ab,A}	56 ± 2 ^{ab,A}	22 ± 2 ^{c,A}
	ASH	16 ± 3 ^{b,B}	54 ± 3 ^{b,A}	38 ± 3 ^{bc,A}

A: alginate; S: sucrose; GG: guar gum; AG: arabic gum; L: low methoxyl pectin; H: high methoxyl pectin. Different lowercase letters on the columns (a − e) indicate significant differences between systems of the same extract ($p < 0.05$). Different capital letters on the columns (A-B) indicate significant differences between extracts on the same bead system ($p < 0.05$).

parameters. When the analysis of variance indicates differences among means, a *t*-test was used to differentiate means with 95% of confidence ($p < 0.05$).

3. Results and discussion

3.1. Hydrocolloids effect on encapsulated betacyanins and polyphenols

Aqueous extracts were obtained from leaves and stems of beetroot as optimized in a previous work (Aguirre-Calvo et al., 2018). The leaf extract contained 6.0 ± 0.2 $g{\cdot}L^{-1}$ of betacyanin (BC) and 0.43 ± 0.02 $g_{\text{gallic acid equivalents}}{\cdot}L^{-1}$ of polypohenols (TP). Stem extracts have greater BC content (40.6 ± 0.9 $g_{\text{betacyanin}}{\cdot}L^{-1}$) and lower content of TP (0.17 ± 0.03 $g_{\text{gallic acid equivalents}}{\cdot}L^{-1}$). Both extracts were encapsulated in Ca(II)-alginate beads with sucrose and pectins or gums. Table 2 shows the loading efficiencies of BC and TP and the remaining antioxidant activity of ABTS (RAA). Beads containing sucrose were used as the baseline systems, since it was already established that its inclusion enhanced the loading efficiencies of the co-encapsulated compounds (Aguirre-Calvo et al., 2018). Loading efficiency of BC for leaf extract was higher than in stem extract, although the absolute content values of BC for stem (between 1.71 and 4.14 $g.L^{-1}$) was approximately 3.5 times higher than leaf (between 0.59 and 1.33 $g.L^{-1}$), as showed in Table S1 of the Supplementary File. This higher content was also evidenced by direct observation of beads color. Conversely, loading efficiency for TP of stem extract was higher than leaf extract, but the beads containing the later extract have 2.7 times more polyphenols (between 0.18 and 0.22 $g_{\text{gallic acid equivalents}}{\cdot}L^{-1}$) than those with stem extract (between 0.05 and 0.08 $g_{\text{gallic acid equivalents}}{\cdot}L^{-1}$), as reported in Table S1 of the Supplementary File. Beads containing stem extract showed higher remaining antioxidant activity (RAA) than those containing leaf extract regardless of the bead composition, as expected by the TP loading efficiency.

Addition of guar gum showed an important effect on entrapment of BC and TP regardless of the encapsulated extract. However, when analyzing the RAA for these systems, although both present the higher values, only the beads with stem extract showed a significant increment by guar gum addition.

All gums increased BC loading efficiency for stem extract, but almost no significant differences were observed for TP, with even lower values in the presence of arabic gum.

Both low and high methoxyl pectins showed severe reductions on the RAA of beads containing any of the extracts. These changes can be related to the presence of the additional polygalacturonate groups that can interact directly with the TP and BC, as well as by promoting modifications of Ca(II)-alginate associations forming the network, as will be further analyzed.

3.2. Hydrocolloids effect on Ca(II)-alginate bead structure

Fig. 1 shows the intensity plots as a function of the scattering vector (q) derived from SAXS experiments for representative samples of Ca(II)-alginate hydrogels containing sucrose (AS) in the presence of the extracts or without them (Fig. 1A) and for samples with all the co-polymers without extracts (Fig. 1B). From these plots, several relevant parameters can be obtained to evaluate both the molecular and supramolecular structure formed within the Ca(II)-alginate network. This network is modeled as a mass fractal system and the scattering curve is divided into three regions, which allow the characterization of the system at different length scales. The interconnectivity of the rods that build up the alginate network (parameter α_1) can be obtained from the slope of the power law at values of $q < 0.28\,nm^{-1}$. For intermediate values of q ($0.55\,nm^{-1} < q < 1.5\,nm^{-1}$), the slope (parameter α_2) represents the compactness within the rods, and the slope for values of $q > 1.5\,nm^{-1}$ (parameter α_3) characterizes the interconnectivity of the basic units that built up the rod (alginate dimers). The intersection of α_1 and α_2 gives the radii of gyration of the rods (R_1), and the intersection of α_2 and α_3 corresponds to the outer radius of the dimers inside the rods (R_2). The last two parameters were evaluated from the maximum or minimum values of the Kratky plot, scattering intensity multiplied by the square modulus of the scattering vector, $I(q).q^2$, as a function of the modulus of q (Aguirre-Calvo et al., 2018; Agulhon, Robitzer, David, & Quignard, 2012).

Starting from the smallest structures observed in the Ca(II)-alginate network, the interconnectivity and size of the alginate dimers that self-associate to compose each rod, α_3 and R_2, respectively, are shown in Fig. 2. As a general trend, there are no significant differences in the interconnectivity by the presence of the extracts, analyzing each system individually. However, the system with high methoxyl pectin (w/o extract) and the system with guar gum in the presence of leaf extract showed an increase in the density of the dimers, revealing specific effects. It is worth noting that this last effect is also linked with the increase in R_2, and it can be correlated to the higher loading efficiency of

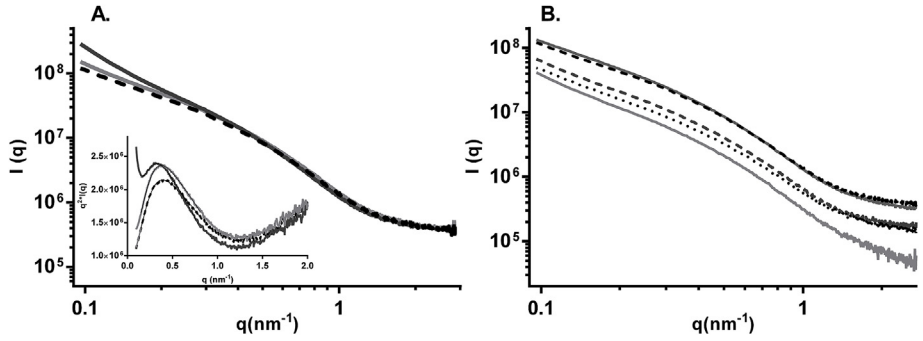

Fig. 1. log–log SAXS profile plots of A. representative Ca(II)-alginate-sucrose (AS) beads loaded with leaf (solid-dark gray curve) and stem (solid-gray curve) extracts and without them (dashed-black curve) and B. Ca(II)-alginate without extracts containing sucrose (dashed-black curve), and sucrose with biopolymers: high methoxyl pectin (solid-dark gray curve); arabic gum (dashed-dark gray curve); guar gum (dotted-black curve); low methoxyl pectin (solid-light gray curve), from top to bottom. Inset in Figure A corresponds to Kratky plot.

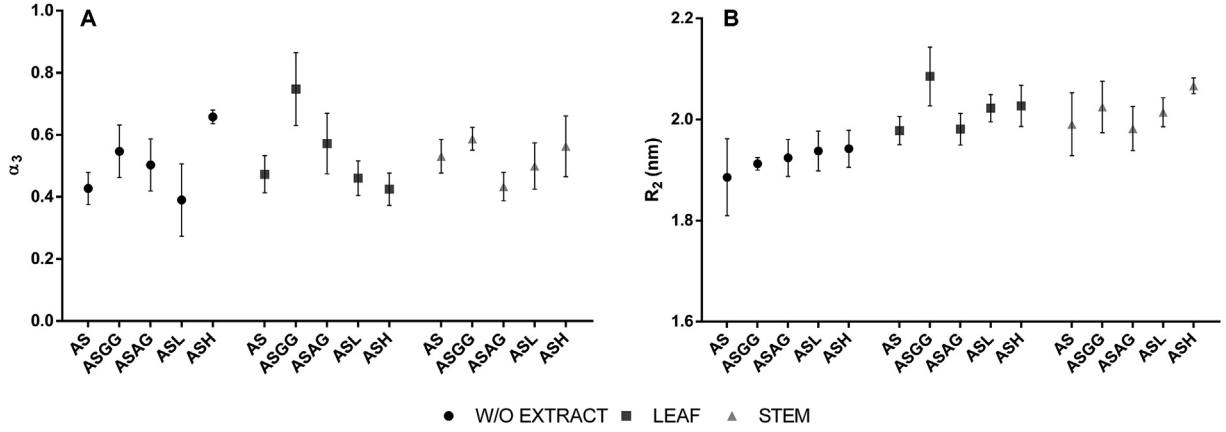

Fig. 2. Microstructure parameters of Ca(II)-alginate beads with and without extract. A. Fractal dimension at distances lower than R_2 defined as parameter α_3 of the microstructure derived from log–log SAXS profiles. B. Characteristic size of the Ca(II)-alginate dimers (R_2) deduced from the minima obtained on Kratky plots. Standard deviations values are included. A: alginate; S: sucrose; GG: guar gum; AG: arabic gum; L: low methoxyl pectin and H: high methoxyl pectin.

TP, indicating that the interactions of the bioactive compounds with their encapsulation matrix can be mediated by the guar gum additive.

Fig. 3 shows parameters α_2 and R_1, representing the compactness and size of the alginate rods. The main effect observed is the size increment of the rod (R_1) promoted by the presence of the leaf extract, which is in line with previous results (Aguirre-Calvo et al., 2018). The structural alterations can be attributed to the presence of trivalent cations in the leaf extract. Particularly, Fe^{3+} concentrations were more than 2 times higher in leaf than in stem (14.4 ± 0.3 and 6.4 ± 0.6 $mg_{Fe^{3+}}/kg_{sample}$, respectively). Compared to divalent cations, trivalent ones offer a more versatile and larger coordination environment, expanding the possible chain arrays within the crosslinked hydrogel, and resulting in a more ramified network as previously reported (Sonego, Santagapita, Perullini, & Jobbágy, 2016; Yang et al., 2013). It is worth noting that the system with arabic gum and leaf extract presented a particularly high value of parameter R_1, indicative of an overly high alginate rod size, suggesting specific interactions between this additive and components of this natural extract. Further studies should be conducted to clarify this issue. On the other hand, the addition of guar gum generates a decrease both in the compactness and size of the rods. This effect can be attributed to the steric hindrance of the guar gum on the alginate polymer chains, causing an impeded diffusion which in turn could result in a more disordered alginate network (decrease in α_2) and a lower multiplicity of the junction zones (lower R_1), in accordance to previous results (Traffano-Schiffo et al., 2017). This in turn can explain the higher entrapment of BC and TP regardless of the encapsulated extract observed in presence of guar gum. Conversely, the addition of both types of pectins does not generate notorious changes in these parameters, suggesting lower interaction with the alginate network at this scale (~10 nm).

At the largest analyzed scale, the level of interconnectivity of the rods (parameter α_1) increased in samples containing leaf extract (Fig. 4), in line with the microstructural changes observed at the intermediate scale (density and size of the alginate rods). In this sense, all the Fe^{3+} present is expected to coordinate triple alginate polymer centers explaining a coordination of carboxylic groups from three different alginate chains, which in turn results in a higher incidence of "tripartite junction nodes". On the other hand, the addition of low methoxyl pectin (L) showed an increase in the interconnectivity of the alginate rod network in the systems without extracts. This effect can be related to the ability of the carboxyl groups of the L to bind Ca^{2+} ions inducing the assembly of the chains and network formation in a similar way than alginate (Schuster, Cucheval, Lundin, & Williams, 2011). However, L possesses an extraordinary more flexible signature than

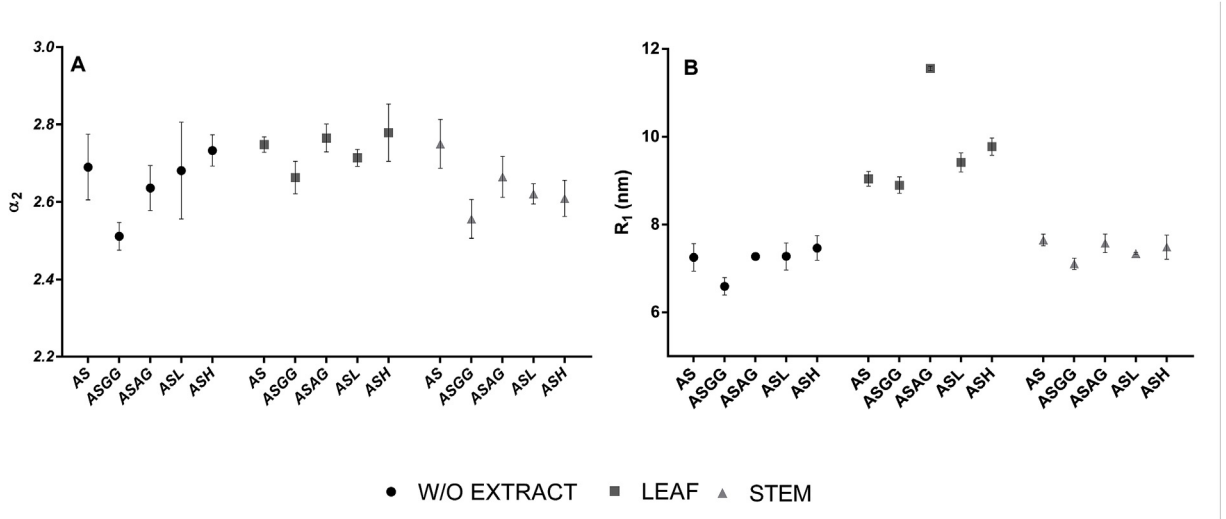

Fig. 3. Microstructure parameters of Ca(II)-alginate beads with and without extract. A. Fractal dimension at distances lower than the characteristic size of the rods or parameter α_2 of the microstructure derived from log–log SAXS profiles. B. Rod cross-sectional radius (R_1) deduced from the maxima obtained on Kratky plots. Standard deviation values are included. A: alginate; S: sucrose; GG: guar gum; AG: arabic gum; L: low methoxyl pectin and H: high methoxyl pectin.

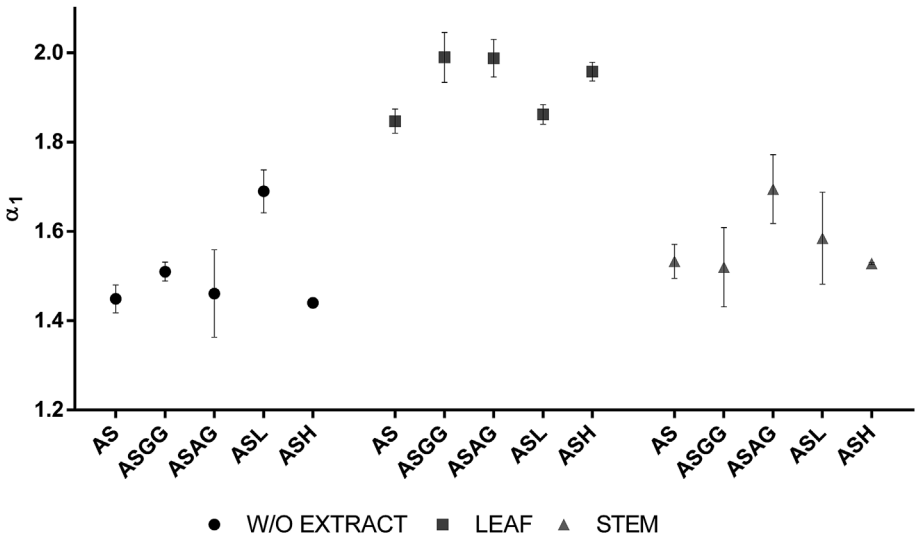

Fig. 4. Microstructure parameters of Ca(II)-alginate beads with and without extract. Fractal dimension of the rod network, parameter α_1 of the microstructure derived from log–log SAXS profiles. Standard deviation values are included. A: alginate; S: sucrose; GG: Guar Gum; AG: Arabic Gum; L: low methoxyl pectin and H: high methoxyl pectin.

alginate, which allows being connected from single-chain sections linked by dimeric associations to network filaments of even 32 chains (Schuster et al., 2011). Even though several consecutive un-methyl-esterified residues (between 8 and 15) are required to form stable junction zones of pectin dimers (Morris, Powell, Gidley, & Rees, 1982), the presence of pectin and its microstructural flexibility offers an extra possibility to coordinate with alginate through Ca^{2+} ions, explaining the observed higher interconnectivity.

Several aspects can be discussed considering the above-presented information. Of the added hydrocolloids, only guar gum produced an increase in the loading efficiency of both betacyanin and polyphenols, increasing also the remaining antioxidant activity (only for stem extract). GG possess higher molecular weight and viscosity than the other employed biopolymers. Besides, it produced changes in the microstructure at the smallest and intermediate scales, affecting both the alginate dimer (increasing it) and the rod size and compactness (decreasing them) as a consequence of the steric hindrance, as previously discussed. As a general rule, arabic gum and both pectins showed poor functional characteristics in both extracts. Even though they all can be used to increase the loading efficiency of betacyanin in stem extract, they reduce the remaining antioxidant capacity. As commented earlier, each of these polymers depicts some special microstructural features in the absence or presence of one type of extract, but none of them maintained these changes through all the experimental conditions, which reveal the plasticity of the different structures generated on each condition. On the other hand, the type of the extract produced strong microstructural effects, related to the content of trivalent cations which offers extra-coordination of alginate chains prior to gelation, being this effect much stronger than any of the changes promoted by the addition of any polymer. Thus, the addition of guar gum seems to be a very good alternative for Ca(II)alginate-sucrose beads production since it increases the functional properties and produces stable microstructural modifications, independently of the employed extract. Conjointly, it was already reported that the inclusion of guar gum maintained the microstructural stability during processing conditions as well as pH changes, as previously demonstrated by Traffano-Schiffo et al. (2018).

4. Conclusion

Typically, the strategy to increase the loading efficiency on Ca(II)-alginate beads was the addition of excipients that have some affinity for the alginate and at the same time for the compounds of interest (bioactives). However, the effect of these excipients in the microstructure of the beads was often shallowed. In the present work, we demonstrate that the presence of hydrocolloids in Ca(II)-alginate beads supplemented with sucrose produced changes at different scales in the 1–100 nm range, affecting from the alginate dimers size and density, the rods size and compactness as well as their interconnectivity. Nevertheless, these modifications can be overlied by the presence of an extract (such as the leaf one), which leads to alginate coordination prior to gelation, strongly affecting the resulting microstructure.

Among the used hydrocolloids, only guar gum achieves the two proposed criteria: increasing functional properties (higher loading efficiencies and remaining antioxidant activity) and consolidating microstructural modulations (on control and independently of the employed extract). Then, the addition of guar gum can lead to Ca(II)-alginate beads with improved properties which constitute a promising enhancement in terms of stability under processing conditions for ingredients used on functional foods.

Conflicts of interest

The author declares that there is no conflict of interests regarding the publication of this paper.

Acknowledgements

This work was supported by the Brazilian Synchrotron Light Laboratory (LNLS, Brazil, proposals SAXS1-20160278 and SAXS1-20170213), Universidad de Buenos Aires (UBACyT 20020130100610BA), Agencia Nacional de Promoción Científica y Tecnológica (ANPCyT PICT 2012-3070), CIN-CONICET (PDTS 2015-196), and CONICET.

Appendix A. Supplementary data

Supplementary data to this article can be found online at https://doi.org/10.1016/j.lwt.2019.05.047.

References

Aguirre Calvo, T. R., Busch, V. M., & Santagapita, P. R. (2017). Stability and release of an encapsulated solvent-free lycopene extract in alginate-based beads. *Lebensmittel-Wissenschaft und -Technologie- Food Science and Technology, 77*, 406–412.

Aguirre Calvo, T., & Santagapita, P. (2016). Physicochemical characterization of alginate beads containing sugars and biopolymers. *Journal of Quality and Reliability Engineering, 2016*, 9184039. 7 pages https://doi.org/10.1155/2016/9184039.

Aguirre-Calvo, T. R., Perullini, A. M., & Santagapita, P. R. (2018). Encapsulation of betacyanins and polyphenols extracted from leaves and stems of beetroot in Ca(II)-alginate beads: A structural study. *Journal of Food Engineering, 235*, 32–40.

Agulhon, P., Robitzer, M., David, L., & Quignard, F. (2012). Structural regime identification in ionotropic alginate gels: Influence of the cation nature and alginate

structure. *Biomacromolecules, 13*(1), 215–220.
Amaral, A. S., Anghinoni, I., & Deschamps, F. C. (2004). Resíduo de plantas de cobertura e mobilidade dos produtos da dissolução do calcário aplicado na superfície do solo. *Revista Brasileira de Ciência do Solo, 28*(1), 115–123.
Baiano, A. (2014). Recovery of biomolecules from food wastes-a review. *Molecules, 19*, 14821–14842.
Baiao, D. D. S., de Freitas, C. S., Gomes, L. P., da Silva, D., Correa, A., Pereira, P. R., et al. (2017). Polyphenols from root, tubercles and grains cropped in Brazil: Chemical and nutritional characterization and their effects on human health and diseases. *Nutrients, 9*, 1044.
Bekhit, M., Arab-Tehrany, E., Kahn, C. J. F., Cleymand, F., Fleutot, S., Desobry, S., et al. (2018). Bioactive films containing alginate-pectin composite microbeads with lactococcus lactis subsp. lactis: Physicochemical characterization and antilisterial activity. *International Journal of Molecular Sciences, 19*, 574.
Campelo, P. H., Junqueira, L. A., Resende, J. V. D., Zacarias, R. D., Fernandes, R. V. D. B., Botrel, D. A., et al. (2017). Stability of lime essential oil emulsion prepared using biopolymers and ultra-sound treatment. *International Journal of Food Properties, 20*, S564–S579.
Chawda, P. J., Shi, J., Xue, S., & Young Quek, S. (2017). Co-encapsulation of bioactives for food applications. *Food Quality and Safety, 1*(4), 302–309.
Chemteach (2019). University of Canterburyhttp://www.chemteach.ac.nz/investigations/investigations.shtml, Accessed date: 29 April 2019 Accessed.
Cheng, Y., Brown, K. M., & Prud'homme, R. K. (2002). Characterization and intermolecular interactions of hydroxypropyl guar solutions. *Biomacromolecules, 3*, 456–461.
Ćujić, N., Trifković, K., Bugarski, B., Ibrić, S., Pljevljakušić, D., & Šavikin, K. (2016). Chokeberry (*Aronia melanocarpa L.*) extract loaded in alginate and alginate/inulin system. *Industrial Crops and Products, 86*, 120–131.
Day, L., Seymour, R. B., Pitts, K. F., Konczak, I., & Lundin, L. (2009). Incorporation of functional ingredients into foods. *Trends in Food Science & Technology, 20*, 388–395.
Deladino, L., Navarro, A. S., & Martino, M. N. (2013). Carrier systems for yerba mate extract (*Ilex paraguariensis*) to enrich instant soups. *Release mechanisms under different pH conditions LWT - Food Science and Technology, 53*(1), 163–169.
Galanakis, C. M. (2012). Recovery of high added-value components from food wastes: Conventional, emerging technologies and commercialized applications. *Trends in Food Science & Technology, 26*(2), 68–87.
George, M., & Abraham, T. E. (2007). pH sensitive alginate–guar gum hydrogel for the controlled delivery of protein drugs. *International Journal of Pharmaceutics, 335*, 123–129.
Gómez-Díaz, D., Navaza, J. M., & Quintáns-Riveiro, L. C. (2008). Intrinsic viscosity and flow behaviour of Arabic gum aqueous solutions. *International Journal of Food Properties, 11*, 773–780.
Guo, J., Giusti, M. M., & Kaletunç, G. (2018). Encapsulation of purple corn and blueberry extracts in alginate-pectin hydrogel particles: Impact of processing and storage parameters on encapsulation efficiency. *Food Research International, 107*, 414–422.
Jackman, R. L., & Smith, J. L. (1996). Anthocyanins and betalains. In G. A. F. Hendry, & J. D. Houghton (Eds.). *Natural food colorants* (pp. 244–309). London: Chapman.
Krishnaiah, Y. S. R., Karthikeyan, R. S., & Satyanarayana, V. (2002). A three-layer guar gum matrix tablet formulation for oral controlled delivery of highly soluble metoprolol tartrate. *International Journal of Pharmaceutics, 241*, 353–366.
Kumar, K., Yadav, A. N., Kumar, V., Vyas, P., & Dhaliwal, H. S. (2017). Food waste: A potential bioresource for extraction of nutraceuticals and bioactive compounds. *Bioresour Bioprocess, 4*(1), 18.
Mello, D. F., Franzolini, R., Fernandes, L. B., Franco, A. V. M., & Alves, T. C. (2008). Avaliação do resíduo de nabo forrageiro extraído da produção de biodiesel como suplemento para bovinos de corte em pastagens. *Revista Brasileira de Saúde e Produçao Animal, 9*(1), 45–56.
Morris, E. R., Powell, D. A., Gidley, M. J., & Rees, D. A. (1982). Conformations and interactions of pectins. I. Polymorphism between gel and solid states of calcium polygalacturonate. *Journal of Molecular Biology, 155*(4), 507–516.
Nami, Y., Haghshenas, B., & Yari Khosroushahi, A. (2016). Effect of psyllium and gum Arabic biopolymers on the survival rate and storage stability in yogurt of *Enterococcus durans* IW3 encapsulated in alginate. *Food Sciences and Nutrition,* 1–10.
Nayak, A. K., Das, B., & Maji, R. (2012). Calcium alginate/gum Arabic beads containing glibenclamide: Development and in vitro characterization. *International Journal of Biological Macromolecules, 51*(5), 1070–1078.
Opanasopit, P., Apirakaramwong, A., Ngawhirunpat, T., Rojanarata, T., & Ruktanonchai, U. (2008). Development and characterization of pectinate micro/nanoparticles for gene delivery. *AAPS- Pharmaceutical science and technology, 9*, 67–74.
Pal, A., Giri, A., & Bandyopadhyay, A. (2016). Influence of hydrodynamic size and zeta potential of a novel polyelectrolyte poly(acrylic acid) grafted guar gum for adsorption of Pb(II) from acidic waste water. *Journal of Environment and Chemistry Engineering, 4*, 1731–1742.
Quintanilla-Carvajal, M., Camacho-Diaz, B., Meraz-Torres, S., Chanona-Peréz, J., Alamilla-Beltran, L., Jimenéz-Aparicio, A., et al. (2010). Nanoencapsulation: A new trend in food engineering processing. *Food Engineering Reviews,* (2), 39–50 1.
Re, R., Pellegrini, N., Proteggente, A., Pannala, A., Yang, M., & R.E (1999). Antioxidant activity applying an improved ABTS radical cation decolorization assay. *Free Radical Biology and Medicine, 26*(98), 1231–1237.
Santagapita, P. R., Mazzobre, M. F., & Buera, M. P. (2011). Formulation and drying of alginate beads for controlled release and stabilization of invertase. *Biomacromolecules, 12*(9), 3147–3155.
Sawicki, T., & Wiczkowski, W. (2018). The effects of boiling and fermentation on betalain profiles and antioxidant capacities of red beetroot products. *Food Chemistry, 259*, 292–303.
Sayah, M. Y., Chabir, R., Benyahia, H., Rodi-Kandri, Y., Ouazzani-Chahdi, F., Touzani, H., et al. (2016). Yield, esterification and molecular weight evaluation of pectins isolated from orange and grapefruit peels under different conditions. *PLoS One, 11*(9), 1–16.
Schuster, E., Cucheval, A., Lundin, L., & Williams, M. A. K. (2011). Using SAXS to reveal the degree of bundling in the polysaccharide junction zones of microrheologically distinct pectin gels. *Biomacromolecules, 12*, 2583–2590.
Silveira, S., Daroit, D., & Brandelli, A. (2008). Pigment production by *Monascus purpureus* in grape waste using factorial design. *LWT-Food Science Technology, 41*(1), 170–174.
Sonego, J. M., Santagapita, P. R., Perullini, M., & Jobbágy, M. (2016). Ca(II) and Ce(III) homogeneous alginate hydrogels from the parent alginic acid precursor: A structural study. *Dalton Transactions, 45*(24), 10050–10057.
Thu, B., Gåserød, O., Paus, D., Mikkelsen, A., Skjåk-Bræk, G., Toffanin, R., et al. (2000). Inhomogeneous alginate gel spheres: An assessment of the polymer gradients by synchrotron radiation-induced x-ray emission, magnetic resonance microimaging, and mathematical modeling. *Biopolymers, 53*(1), 60–71.
Traffano-Schiffo, M. V., Aguirre Calvo, T. R., Castro-Giraldez, M., Fito, P. J., & Santagapita, P. R. (2017). Alginate beads containing lactase: Stability and microstructure. *Biomacromolecules, 18*(6), 1785–1792.
Traffano-Schiffo, M. V., Castro-Giraldez, M., Fito, P. J., Perullini, M., & Santagapita, P. R. (2018). Gums induced microstructure stability in Ca(II)-alginate beads containing lactase analyzed by SAXS. *Carbohydrate Polymers, 179*, 402–407.
Tsai, F. H., Kitamura, Y., & Kokawa, M. (2017). Effect of gum Arabic-modified alginate on physicochemical properties, release kinetics, and storage stability of liquid-core hydrogel beads. *Carbohydrate Polymers, 174*, 1069–1077.
Vicini, S., Castellano, M., Mauri, M., & Marsano, E. (2015). Gelling process for sodium alginate: New technical approach by using calcium rich micro-spheres. *Carbohydrate Polymers, 134*, 767–774.
Wandrey, C., Bartkowiak, A., & Harding, S. (2010). Materials for encapsulation. *Encapsulation Technologies for active food Ingredients and food processing* (pp. 31–100). New York: Springer.
Wilkins, M. R., Widmer, W. W., Grohmann, K., & Cameron, R. G. (2007). Hydrolysis of grapefruit peel waste with cellulase and pectinase enzymes. *Bioresource Technology, 98*(8), 1596–1601.
Wootton-Beard, P. C., Moran, A., & Ryan, L. (2011). Stability of the total antioxidant capacity and total polyphenol content of 23 commercially available vegetable juices before and after in vitro digestion measured by FRAP, DPPH, ABTS and Folin-Ciocalteu methods. *Food Research International, 44*(1), 217–224.
Wu, T., Huang, J., Jiang, Y., Hu, Y., Ye, X., Liu, D., et al. (2018). Formation of hydrogels based on chitosan/alginate for the delivery of lysozyme and their antibacterial activity. *Food Chemistry, 240*, 361–369.
Yang, C. H., Wang, M. X., Haider, H., Yang, J. H., Sun, J. S., Chen, Y. M., et al. (2013). Strengthening alginate/polyacrylamide hydrogels using various multivalent cations. *ACS Applied Materials & Interfaces, 5*(21), 10418–10422.
Yapo, B., & Koffi, K. (2013). Extraction and characterization of highly gelling low methoxy pectin from cashew apple pomace. *Foods, 3*, 1–12.
Zhao, G. Y., Diao, H. J., & Zong, W. (2013). Nature of pectin–protein–cathechin interactions in model systems: Pectin–protein–cathechin interactions. *Food Science and Technology International, 19*, 153–165.